

(presented at the 1999 NCSL Workshop & Symposium, Charlotte, NC)

## **Primary Acoustic Thermometry up to 800 K**

Presenter: D. C. Ripple

National Institute of Standards and Technology (NIST), 100 Bureau Dr., Stop 8363,  
Gaithersburg, MD 20899-8363 (301) 975-4801 (Tel.), (301) 548-0206 (Fax)

Paper Authors: D. C. Ripple, D. R. Defibaugh, K. A. Gillis, and M. R. Moldover  
National Institute of Standards and Technology, Gaithersburg, MD 20899

### **Abstract**

Primary acoustic thermometers determine the thermodynamic temperature of a monatomic gas from measurements of the speed of sound in the gas. Here, we describe the design and construction of an acoustic thermometer designed to operate at temperatures up to 800 K with unprecedented accuracy. Features of our thermometer include: construction that minimizes sources of gas contamination; continuous purging of the resonator; monitoring the purity of the gas by gas chromatography; determination of the resonator's volume by *in situ* measurements of microwave resonance frequencies; use of novel acoustic transducers; and measurement of the resonator's temperature on the International Temperature Scale of 1990 (ITS-90) with removable, long-stem standard platinum resistance thermometers (SPRTs). We are in the process of implementing this thermometer at NIST, and results will be presented at a later date.

## **1. Basic Principles of Primary Gas Thermometers**

### **1.1 Thermodynamic Temperature**

The physical quantity termed temperature is not an arbitrary measure of the degree of hotness of an object. Temperature is well-defined by the laws of thermodynamics, and measures of temperature that are defined to be consistent with the laws of thermodynamics are said to be thermodynamic temperatures or are said to be on a thermodynamic scale. Experimental measurements of thermodynamic temperatures, using primary thermometers, form the basis for such temperature scales as the ITS-90.

The definition of the Kelvin Thermodynamic Temperature Scale in the SI system of units states that the triple point of water is 273.16 K and absolute zero is 0 K, exactly. Other values of temperature on this scale are defined by requiring that the temperature values must be consistent with the laws of thermodynamics.

In practice, thermometers are not calibrated at 0 K and 273.16 K, and the thermodynamic behavior of laboratory thermometers is not understood to high accuracy. Instead, thermometers

are calibrated on a convenient, practical scale that approximates the thermodynamic temperature scale to the highest possible accuracy. The most recent scale designed for general use is the ITS-90. In this paper, we will use  $T$  to denote temperatures on the Kelvin Thermodynamic Temperature Scale and  $T_{90}$  to denote temperatures on the ITS-90.

It is possible to construct a thermometer that measures thermodynamic temperature. One first chooses a physical system that can be created in the laboratory and whose temperature is related to a set of measurable properties. By measurement of this set of properties, the thermodynamic temperature of the system is determined. Examples are discussed in sections 1.2 and 1.3. The difference between temperatures on the ITS-90 and the thermodynamic temperature scale can be determined by placing laboratory thermometers calibrated on the ITS-90 in the same apparatus that is used to determine  $T$ . Once the difference between  $T_{90}$  and  $T$  is known, this information can be used to improve future versions of the international temperature scales.

## 1.2 Primary Constant Volume Gas Thermometers

From 273.16 K (0.01 °C) to 730 K (429.85 °C), the ITS-90 is based on thermodynamic temperature measurements that use a monatomic gas and the ideal gas law<sup>(1)</sup>:  $pV = nRT$ , where  $p$  is the gas pressure,  $V$  is the volume of a closed vessel,  $n$  is the number of moles, and  $R$  is the gas constant. A straightforward method of determining  $T$  through this equation is to keep  $V$  fixed and to determine the ratio of pressures at an unknown temperature to the pressure at the triple point of water:

$$\frac{T}{273.16 \text{ K}} = \frac{p(T)}{p(273.16 \text{ K})} \quad (1)$$

This method is termed Constant Volume Gas Thermometry (CVGT)

Unfortunately, the best previous measurements<sup>(2,3)</sup> using CVGT have discrepancies of 12 mK at 500 K and rising to 30 mK at 730 K, which are much larger than the combined measurement uncertainty. Major limitations of this method include the necessity of maintaining both a pure gas sample and a predictable volume for the time necessary to measure  $p$  at both the unknown temperature and at the triple point of water.

## 1.3 Primary Acoustic Thermometers

An alternative type of gas thermometer is the acoustic thermometer, which again relies on a simple relationship between thermodynamic temperature and measurable properties of the gas. The property to be measured in this case is the speed of sound of a monatomic gas,  $u$ . In the limit of zero gas density, the dependence of  $u$  on  $T$  is given by:

$$mu^2 = \gamma k_B T, \quad (2)$$

where  $m$  is the mass of one molecule,  $\gamma$  is the specific heat ratio, and  $k_B$  is Boltzmann's constant. For the monatomic gases,  $\gamma = 5/3$ . The thermodynamic temperature can be expressed in terms of the ratio of  $u$  at that temperature to  $u$  at the triple point of water:

$$\frac{T}{273.16 \text{ K}} = \left[ \frac{u(T)}{u(273.16 \text{ K})} \right]^2 \quad (3)$$

As shown in Fig. 1, recent acoustic thermometry results<sup>(4)</sup> at NIST have determined thermodynamic temperature with a standard uncertainty of 0.6 mK in the temperature range 217 K to 303 K. The discrepancies of the CVGT work and the recent success at measuring thermodynamic temperatures near 270 K with an acoustic thermometer motivated us to develop an acoustic thermometer for determining the thermodynamic temperature above 500 K.

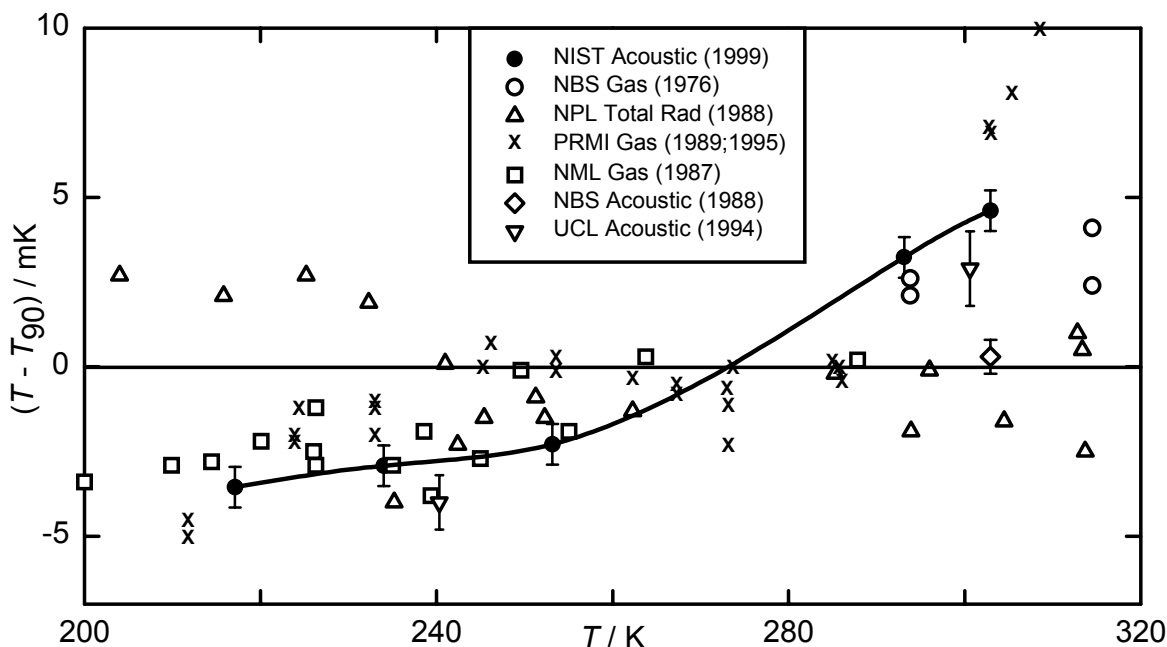


Figure 1. The difference between recent determinations of thermodynamic temperature and  $T_{90}$ .

In the NIST thermometer, the speed of sound of a monatomic gas (argon or xenon, typically) is determined from measurements of the frequencies of acoustic resonances in a gas-filled spherical shell of volume  $V$  and radius  $a$ . Typical frequencies measured for thermometry purposes vary from 2.5 kHz to approximately 18 kHz for a spherical resonator with a 3 L volume. For any particular resonance mode, the resonance frequencies are proportional to the ratio of the speed of sound to the radius of the resonator cavity,  $u/a$ . In a spherical cavity, there are distinct resonances, or acoustic modes, at certain frequencies labeled  $f_{ln}$ , with  $l=0, 1, \dots$  and  $n=2, 3, \dots$ . The preferred modes for measurement of the speed of sound are those with  $l=0$ , which are termed radial modes. In these modes, the gas moves along a radial path, traveling toward and then away from the inside surface of the shell; there is no component of the gas velocity parallel to the shell surface, as found in other modes. The radial modes have three advantages compared with other modes:

1. For the radial modes, there are generally no other modes with nearly the same frequency. Consequently the analysis to find the frequency  $f_{0n}$  is simple. In contrast, the nonradial modes with  $l=1$  or higher are degenerate, meaning that there is a multiplet of  $2l+1$  modes with nearly the same frequency  $f_{ln}$ . The analysis to find the center frequencies of these overlapping, partially-resolved modes is difficult.

2. Because the flow of the radial modes is radial, there are no viscous losses at the surface, and consequently the resonance frequencies are as distinct as possible.
3. If the spherical shell is deformed from a perfect sphere, the shifts in frequency of the radial modes depend only on the change of volume of the resonator cavity, and not on the details of the deformation.

Measurements of the frequencies of microwave resonances within the same resonator cavity determine the thermal expansion of the cavity<sup>(5)</sup>. The measured acoustic frequencies are proportional to  $u/a$ , and the measured microwave frequencies are proportional to  $a$ . Using Eq. 3, the equation linking the measured frequencies to  $T$ , neglecting small corrections<sup>(4)</sup>, can be found:

$$\frac{T}{T_w} = \left[ \frac{u(T)}{u(T_w)} \right]^2 = \left[ \frac{V(T)}{V(T_w)} \right]^{2/3} \left[ \frac{f_a(T)}{f_a(T_w)} \right]^2 = \left[ \frac{f_m(T_w)}{f_m(T)} \right]^2 \left[ \frac{f_a(T)}{f_a(T_w)} \right]^2, \quad (4)$$

where  $T_w$  is the triple point of water, 273.16 K, and  $f_a$  and  $f_m$  are acoustic and microwave resonance frequencies for a particular choice of modes.

To measure the resonance frequencies of the spherical resonator, a sound wave at a frequency  $f$  is excited in the gas by a small speaker mounted in the shell wall. If the frequency  $f$  matches one of the frequencies  $f_n$ , an acoustic resonance is excited, and the amplitude of the gas motion and pressure oscillations inside the resonator cavity will increase dramatically. Typically, an acoustic detector monitors pressure oscillations inside the shell at the same frequency as the excitation frequency. When the excitation frequency is scanned across the resonance frequency, a well-defined peak is seen in the signal measured by the detector transducer. An example of such a scan is shown in Fig. 2. The shape of the acoustic resonance is well understood, and with a typical acoustic signal, the center frequency of the peak can be determined with a relative uncertainty of the order of  $10^{-6}$ .

Equation 4 neglects the departure of the gas from ideality at non-zero gas density (CVGT is affected in a similar manner) and at the thermal boundary layer in the gas where it contacts the

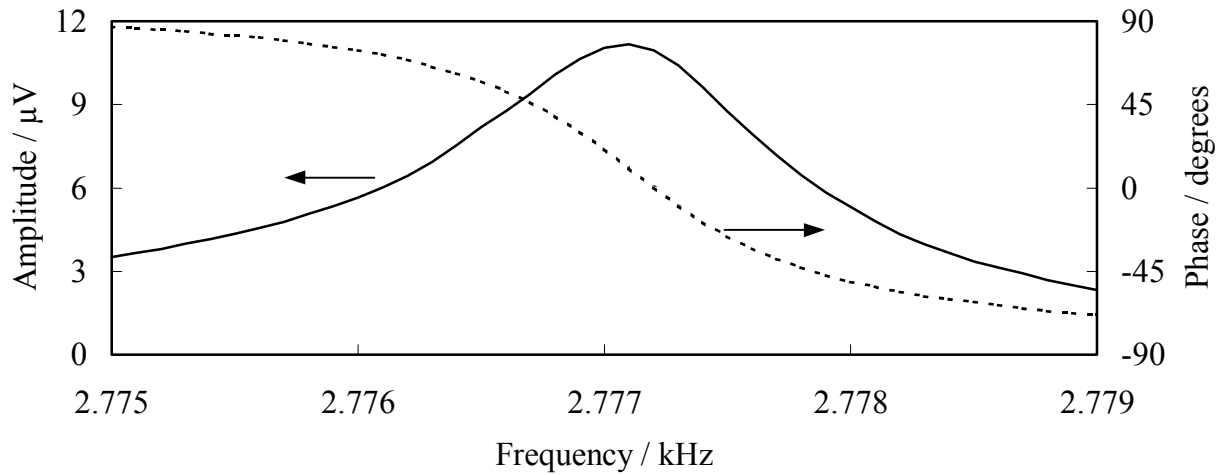


Figure 2. A scan of an acoustic resonance

cavity wall. In practice, the zero-density limit of the speed of sound is found by measuring  $u$  as a function of pressure, and extrapolating to zero pressure. Corrections for the thermal boundary layer are small (fractional shifts of the order  $10^{-4}$  of the frequency, typically), and these shifts can be either calculated from the known thermal properties of the monatomic gas and resonator shell or from analysis of the acoustic measurements. Because the non-ideality increases at high density and the boundary layer corrections increase at low density, there is an optimum range of density that is used in primary acoustic thermometers. For argon in the NIST thermometer, this optimum density will be  $0.02 \text{ mol/dm}^3$  to  $0.2 \text{ mol/dm}^3$ .

Unlike CVGT apparatuses, the measurements of  $f_a$  and  $f_m$  do not require maintaining the same gas in the volume  $V$  during an extended period. The measurements may be made while continuously purging the resonator cavity with new gas. Additional advantages of acoustic thermometry are its inherently high precision and the ability to use microwave resonances to characterize the volume of the resonator cavity *in situ*. A simple schematic of an acoustic thermometer with these features is shown in Fig. 3. The pressure vessel is filled with the same gas as used inside the resonator and at nearly the same pressure, to minimize contamination of the gas in the resonator and to avoid pressure deformations of the spherical shell. The thermal enclosure maintains the spherical resonator at a uniform and constant temperature.

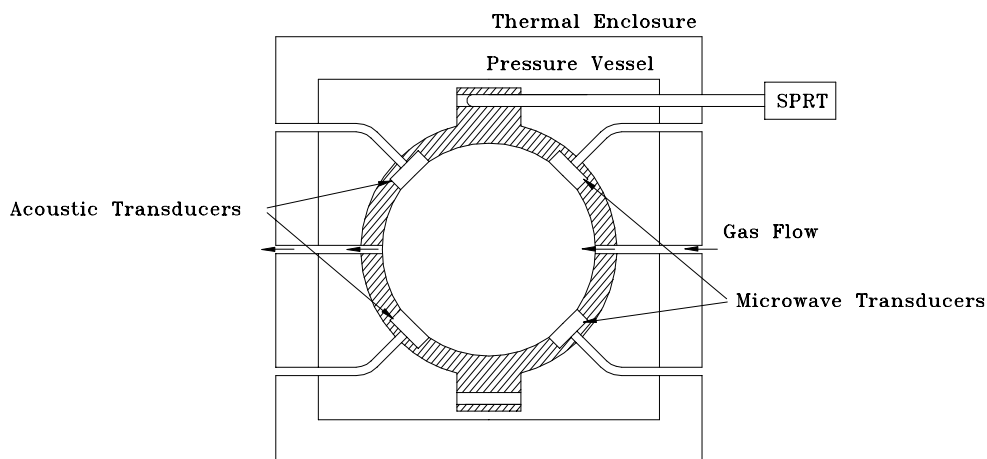


Figure 3. Diagram of the general features of an acoustic thermometer.

## 2. The NIST Acoustic Thermometer

### 2.1 Design Philosophy

The present NIST effort seeks to greatly expand the temperature range of precision acoustic thermometry and to benefit from the lessons learned while conducting the lower temperature measurements. The NIST acoustic thermometer, which is shown in cross section in Fig. 4, has the following features:

- A. Operation up to 800 K. Discrepancies between the NBS/NIST CVGT data become significant at temperatures above 500 K. Measurements at the zinc freezing point (692.677 K) are desirable, because the determined value of  $(T - T_{90})$  at the fixed-point temperatures does not depend on the nonuniqueness of the SPRTs, which is a measure of the interpolation error between fixed points on the ITS-90.
- B. Continuous purging of the resonator cavity. Outgassing from the thermometer materials or permeation of the laboratory air into the thermometer may lead to impurities such as hydrogen or water in the gas in the resonator. Contamination of the gas in the resonator is proportional to its residence time, or inversely proportional to flow rate. Continuous purging reduces gas residence time approximately two orders of magnitude relative to the residence time in CVGT measurements.
- C. Direct measurement of impurities in the gas exiting the resonator.

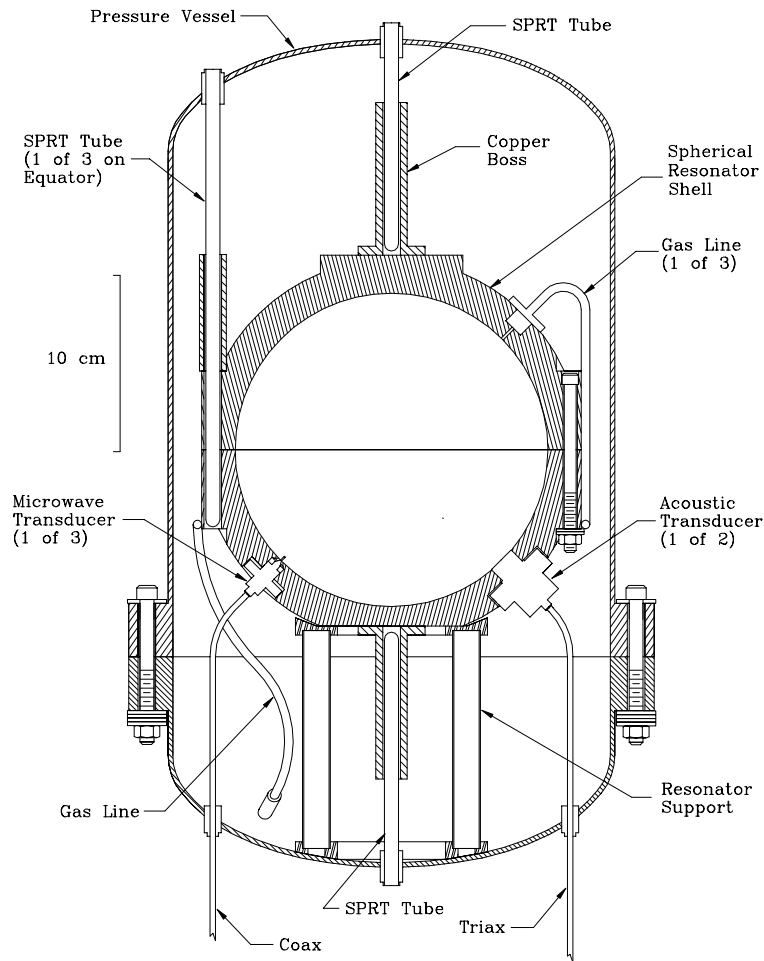


Figure 4. Simplified cross section of the resonator, the pressure vessel, and associated plumbing and electrical connections. The furnace surrounding the pressure vessel is not shown.

- D. Simultaneous microwave and acoustic measurements. At elevated temperatures, creep of the spherical shell is a significant possibility. Microwave measurements that are concurrent with the acoustic measurements test for creep at each datum point.
- E. Stable and inert materials. The thermometer utilizes no elastomers, which have been a significant source of outgassing in previous acoustic thermometers.
- F. Removable thermometers calibrated on the ITS-90. Removable thermometers allow periodic checks at  $T_w$  and easier determination of thermal gradients.
- G. A resonator cavity of approximately 3 L. Previous measurements with cavity volumes of 1 L or less have halfwidths of the acoustic resonances that are larger than predicted by theory.

## 2.2 Materials for high temperature operation

All components of the NIST acoustic thermometer are constructed of materials that are dimensionally stable at 800 K and that have inherently low outgassing rates. The materials exposed to high temperatures include: stainless steel (SS), copper, alumina, boron nitride, platinum, and gold.

The choice of a material for the spherical shell itself requires consideration of additional properties. For instance, the resonator cavity must maintain a nearly spherical shape at all temperatures, and any oxide layer on the cavity wall must be stable. Independent experiments confirmed that copper, 316L stainless steel, nickel 201, and monel all had adequate dimensional and chemical stability, so secondary considerations determined the choice of material for the spherical shell. Because ferromagnetism has undesirable effects on the microwave resonances, nickel was excluded. Monel, and to some extent copper, are difficult to machine in the complicated shapes necessary for the shell halves. Stainless steel has excellent mechanical properties, but poor thermal conductivity. Because calculations demonstrated that thermal conductivity of the shell was not critical, we chose to use the same shell, fabricated from 316L stainless steel, that has been used for previous thermometry work, after modifying it to accommodate new transducers, gas ports, and long-stem SPRTs.

## 2.3 Acoustic measurements with continuous gas flow

There are three requirements when making acoustic measurements with continuous gas flow: (a) the pressure must be sufficiently stable that adiabatic temperature variations in the gas are small, (b) the difference between the temperatures of the gas and of the shell wall must be small, and (c) the gas line must not significantly perturb the acoustic resonances.

A fractional change in gas pressure,  $\Delta p/p$ , will induce an adiabatic change in the gas temperature,  $\Delta T$ , inside the resonator cavity. Requiring temperature stability of 0.5 mK at 800 K leads to the requirement of a fractional pressure stability of  $1.6 < 10^{-6}$  for time scales shorter than the thermal diffusion time of the gas in the resonator cavity, approximately 100 s. We have achieved stabilities substantially better than this with a two stage pressure regulation system upstream of the spherical shell. The gas pressure is first regulated with a standard diaphragm-type regulator. To enable a very fine adjustment of the flow rate, gas flowing from the regulator is then split,

with approximately 90% of the gas flowing through a capillary tube and the remaining 10% of the gas flowing through an electromagnetic flow-control valve. A PID loop adjusts flow through the control valve to maintain a constant pressure of the gas in the resonator. Typical flow rates for our thermometer are  $3 \times 10^{-5}$  mol/s to  $3 \times 10^{-4}$  mol/s.

Thermal equilibrium of the gas with the walls of the spherical shell is attained by straightforward techniques of thermally anchoring the gas lines to two of the shells of the furnace, and to the equatorial region of the spherical shell.

The aperture of the gas line into the spherical shell must be large enough that the gas flow does not become highly turbulent and consequently generate acoustic noise. A large aperture, however, can acoustically couple the resonance volume to the gas line. As suggested in Ref. (6), each gas line opens into a volume of approximately  $1 \text{ cm}^3$  at the wall of the spherical shell, and a small duct of length 1/10 of the cavity radius connects this volume with the resonator cavity, as shown in the upper right of Fig. 4. This geometry acts as a low-pass acoustic filter, preventing significant shifts of the acoustic resonance frequencies. The gas entrance and exit apertures are not diametrically opposite one another. If they were, inadequate mixing might occur, because at high Reynolds numbers, the gas flows out of the small duct into the resonator cavity as a collimated jet.

## 2.4 Minimization and measurement of gas impurities

Impurities in the gas inside the resonator cavity alter  $u(T)$ , with consequent errors in  $T$ . Therefore, we have designed our apparatus to minimize the quantity of impurities, and we confirm the purity of the gas leaving the resonator by direct measurement of impurities and indirect tests of the effects of impurities.

There are three potential sources of impurities: impurities in the source gas, outgassing from thermometer materials, and permeation of laboratory air through the pressure vessel. The purity of commercially-supplied research grade argon (99.9999%) is sufficient for our needs. The primary concerns are contamination by outgassing of materials in contact with the gas and permeation of laboratory air through the pressure vessel. Gas contamination by outgassing is minimized by constructing virtually all components in contact with the gas from metals and hard-fired ceramics. At 800 K, hydrogen readily permeates stainless steel<sup>(7)</sup>. As a result, the dominant impurity at high temperatures is expected to be hydrogen.

If an impurity is present in the resonator cavity, the resonance frequencies will be shifted by an amount proportional to the impurity concentration. In a continuously purged system contaminated by gas permeation and outgassing, the impurity concentration is inversely proportional to flow rate. The most important test of the presence of impurities, then, is to monitor the resonance frequency of an acoustic mode while varying the flow rate of gas through the resonator cavity.

The purity of the gas exiting the cavity will be verified by routing the exiting gas to a customized gas chromatography system capable of detecting hydrogen, nitrogen, carbon monoxide, carbon dioxide, and hydrocarbons at a level of  $0.3 < 10^{-6}$  mole fraction.

## 2.5 Acoustic and microwave transducers

Excitation and detection of the acoustic modes require acoustic transducers that can operate reliably at 800 K, have noise levels equivalent to approximately  $10^{-5}$  Pa/Hz<sup>1/2</sup>, have a smooth frequency response from 2.5 kHz to approximately 17 kHz, and that do not appreciably perturb the frequencies of the acoustic resonances. For operation at room temperature, the ideal transducers are capacitance microphones, which have a thin membrane spaced approximately 40  $\mu$ m from a back electrode. In the detection mode, sound waves deflect the membrane, altering the capacitance between the two electrodes.

For operation at 800 K, no commercial transducers exist that meet our requirements, so we designed and fabricated our own capacitance transducers, as shown in Fig. 5. The membrane is a square of monocrystalline silicon, approximately 25  $\mu$ m thick. This membrane fits in the well of a photoetched stainless steel disk that also serves as a spacer to maintain a 40  $\mu$ m gap between a back SS electrode and the silicon. The back electrode is set into a ceramic insulator fabricated from machinable alumina. These transducers have low outgassing, good dimensional stability at high temperatures, and a smooth frequency response from 0.5 kHz to 18 kHz.

The total capacitance of the transducer is of the order of only 3 pF. To achieve adequate sensitivity, it is necessary to use triaxial cable from the transducer, out of the furnace, through a hermetic feedthrough, and to the preamplifier. The triaxial cable from the transducer to the seal is constructed from two concentric stainless steel tubes and an inner platinum conductor, all insulated from each other by alumina tubes.

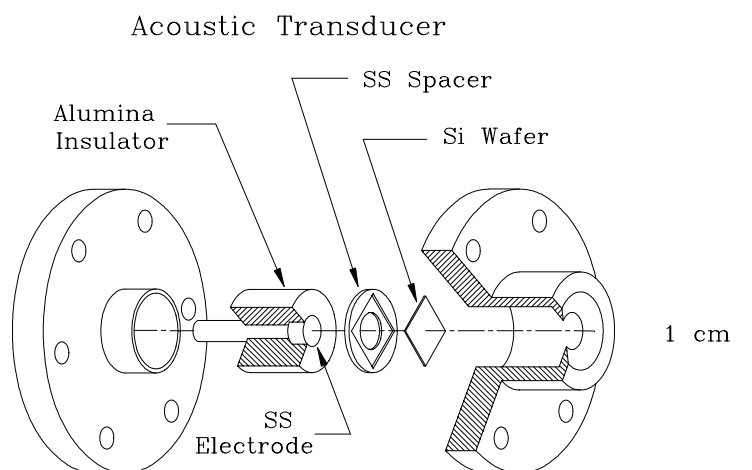


Figure 5. Simplified cross sections of the acoustic transducers.

The variation of the volume of the resonator cavity with temperature is determined from measurements of the center frequencies of microwave resonances as a function of temperature. The microwave resonances are measured with a network analyzer, connected to the spherical shell with homemade, high-temperature coaxial cable terminated at the shell wall with a 3 mm long pin. With this configuration, we are able to measure the resonant frequencies of the three lowest transverse magnetic (TM) triplets at frequencies of 1.47 GHz, 3.28 GHz, and 5.00 GHz with the very small relative uncertainty of approximately  $10^{-7}$ .

The resonant frequency of a given microwave mode is not equally sensitive to all deformations of the resonator cavity. However, it has been shown, theoretically and experimentally<sup>(5)</sup>, that the effective volume for radial acoustic modes is equivalent to the average of the effective volume for all components of a microwave multiplet. The particular cavity of the NIST acoustic thermometer is slightly oblong along the  $z$  axis. Consequently one mode of each TM triplet is split from the other two modes. The doublet cannot be resolved, but it is necessary to insure that the measurements equally weight the two degenerate modes in the determination of the average resonant frequency. This is accomplished by using three transducers, one as a detector and two as a source. The two sources are separated by  $90^\circ$  in the  $x$ - $y$  plane, with one source in the  $x$ - $z$  plane and one in the  $y$ - $z$  plane. From measurements with both sources, the deformations of the resonator cavity can be probed with modes in all three spatial directions:  $x$ ,  $y$ , and  $z$ .

## 2.6 Thermometry on the ITS-90 and the thermal enclosure

Accurate measurements of  $T$  require that the spherical resonator, including the gas in the cavity, be maintained at a uniform and stable temperature. Accurate measurements of  $T_{90}$  additionally require that the SPRTs be in thermal equilibrium with the wall of the spherical shell. To meet these requirements, the pressure vessel is encased in three concentric aluminum shells that are actively temperature controlled, and the thermal coupling between the aluminum shells, the SPRTs, and the spherical resonator have been carefully modeled.

The wall temperature of the spherical shell can be measured with up to five long-stem,  $25.5 \Omega$  SPRTs. As shown in Fig. 4, the pressure vessel has five tubes welded into its walls that slide into copper bosses located at the top, bottom, and equator of the spherical shell. The SPRTs are placed inside these tubes, and the SPRTs may readily be removed while the furnace is at high temperature for the purposes of checking the  $T_w$  resistance ratio or interchanging SPRT positions. Thermal gradients along the SPRT tubes can be mapped by adjusting the SPRT position inside the tubes. As an additional check on the gradients in the shell wall, a differential thermocouple has been installed, with junctions at the equator of the shell and at a position midway between the equator and the top of the shell. The thermocouple has pure Pt leads to room temperature and three Pt/Cu-Ni junctions in series. By annealing the Pt in the same manner as used for Au/Pt thermocouples, the Pt leads introduce no more than  $0.05 \mu\text{V}$  stray thermal emf, equivalent to a 0.5 mK error.

The size of the pressure vessel is determined by the requirement that the SPRTs must have sufficient immersion depth into a region nearly the same temperature as the shell to avoid significant sheath losses. Plots of SPRT response on immersion into zinc freezing-point cells

show that sheath losses are minimal if a 14.5 cm length of the SPRT from the tip is within approximately 10 mK of the sensing element temperature. The resulting pressure vessel is 25.4 cm in diameter and 47 cm long, with elliptical top and bottom ends, and a flange near the bottom end that is sealed with a gold wire o-ring. The aluminum shell surrounding the pressure vessel has a minimum thickness of 1 cm, and additional aluminum bosses are used around the SPRT ports to increase the near-isothermal length of each SPRT to 14.5 cm.

For aluminum shells large enough to encase the pressure vessel, a simple thermal model based on "lump elements" of the thermal resistance of the furnace shell and of the insulation is not appropriate. The design of the furnace must account for the flow of heat both along the shells and across the insulation between shells. A simple analytical model suffices for design purposes and demonstrates that adding control points, each with an independent temperature sensor and heater, is an effective way of improving the thermal uniformity of a furnace. Consider a metal plate of conductivity  $\lambda_m$  and thickness  $d_m$  that is spaced a distance  $d_i$  from a flat substrate by a layer of insulation of thermal conductivity  $\lambda_i$ . If the temperature profile on the substrate varies along its length as  $A_s \sin(kx)$ , then in the limit of  $kd_i \ll 1$  the ratio of the imposed temperature variation on the metal plate to the variation on the substrate is

$$R_{ms} = A_m / A_s = \frac{1}{1 + (k\alpha)^2}, \quad \alpha \equiv \sqrt{\lambda_m d_m d_i / \lambda_i} \quad (5)$$

High values of  $\alpha$  or of  $k$  result in strong attenuation of temperature fluctuations. The strong dependence of  $R_{ms}$  on  $k$  indicates that with several metal shells, the thermal gradients on the innermost shell will be dominated by the spatial fluctuations corresponding to the longest lengths, or the smallest  $k$  values. The variable  $x$  can be imagined to follow a path around the circumference of the shell at its widest dimension. With a shell circumference of  $C$ , and a single temperature control point, the periodicity of the temperature gradients requires  $k=2\pi n/C$ ,  $n=1, 2, \dots$ . Increasing the number of control points to  $N_{cp}$ , and spacing them equally, gives  $k_{min} = 2\pi N_{cp}/C$ . Using this method, we have designed the shells to give a ratio of thermal gradients on the outer aluminum shell to those on the inner shell of 900. The inner and outer shells have three control points each. The gradients on the outermost shell are calculated to be 2 K at a temperature of 800 K, based on the results of numerical calculations.

The accuracy and stability of the temperature of the control points on the innermost aluminum shell is critical for the success of the experiment. We use Au/Pt thermocouples as sensors on the shell. The uncertainty of such sensors is approximately 10 mK, thermocouples made from a single lot of wire are highly interchangeable, and stability tests have indicated no measurable drift for 1000 hours of use at temperatures up to 1235 K. Nanovoltmeters are used to read each Au/Pt thermocouple, and the analog output of each nanovoltmeter is configured to be equal to the amplified difference of the thermocouple emf and a setpoint voltage. The analog output is fed into a standard PID controller that in turn controls the DC power supplies of the shell heaters.

## 2.7 Extension of the Technique to Higher and Lower Temperatures

The temperature range 273 K to 800 K is not a fundamental limit on the technique of acoustic thermometry, but development of an acoustic thermometer capable of measuring temperatures substantially above 800 K would require considerable changes in the thermometer design. A

number of components would need to be constructed of high-nickel alloys, such as Inconel. The furnace shells would need to be constructed from a material with a higher melting point than aluminum, such as a copper-nickel alloy. The spherical resonator of the present thermometer is clamped together with bolts loaded by Inconel disc-spring washers. Finding an alternative to the Inconel springs, which are rated up to 980 K, is a significant challenge. Electrical leakage through the alumina insulator of the acoustic transducers would limit operation as a detector at sufficiently high temperatures.

An acoustic thermometer capable of measuring temperatures substantially below 800 K could readily be built using the same technology as described in this paper, but a smaller resonator may be desirable for greater ease in cooling the apparatus. With the present thermometer and a specialized insulating shell, it may be possible to reach temperatures of approximately 100 K.

## 2.8 Conclusions

The acoustic thermometer described above has been constructed at NIST, and testing of the thermometer is in progress. We anticipate acquiring data over the temperature range 273 K to 800 K, and reporting these results in later publications. From our present understanding of the NIST acoustic thermometer, the standard uncertainties at 800 K are expected to be approximately 3 mK to 5 mK, which will be substantially smaller than the 30 mK discrepancies of CVGT measurements at this temperature.

## References

- (1) Rusby, R. L., Hudson, R. P., Durieux, M., Schooley, J. F., Steur, P. P. M., and Swenson, C. A., "Thermodynamic Basis of the ITS-90," *Metrologia*, **28**, 1992, pp. 9-18
- (2) Guildner, L. A. and Edsinger, R. E., "Deviation of the International Practical Temperatures from Thermodynamic Temperatures in the Temperature Range from 273.16 K to 730 K," *J. Res. Natl. Bur. Stand. (U.S.) Sec. A*, **80**, 1976, pp. 703-737
- (3) Edsinger, R. E. and Schooley, J. F., "Differences between Thermodynamic Temperature and  $t$  (ITS-68) in the Range 230 °C to 660 °C," *Metrologia*, **26**, 1989, pp. 95-106
- (4) Moldover, M. R., Boyes, S. J., Meyer, C. W., and Goodwin, A. R. H., "Thermodynamic Temperatures of the Triple Points of Mercury and Gallium and in the Interval 217 K to 303 K," *J. Res. Natl. Inst. Stand. Technol.*, **104**, 1999, pp. 11-46
- (5) Ewing, M. B., Mehl, J. B., Moldover, M. R. and Trusler, J. P. M., "Microwave Measurements of the thermal expansion of a spherical cavity," *Metrologia*, **25**, 1988, pp. 211-219
- (6) Goodwin, A. R. H., *Thermophysical Properties from the Speed of Sound*, Ph. D. Thesis, University College London, 1988, pp. 113-117
- (7) O'Hanlon, John F., *A User's Guide to Vacuum Technology*, Wiley & Sons, New York, 1980, p. 150